# A Co-axial Scanning Acoustic and Photoacoustic Microscope

Srikant Vaithilingam*, Te-Jen Ma*, Yukio Furukawa*, Adam de la Zerda†, Ömer Oralkan*, Aya Kamaya‡, Shay Keren†, Sanjiv S. Gambhir†, R. Brooke Jeffrey Jr‡ and Butrus T. Khuri-Yakub*
*Edward L. Ginzton Laboratory, Stanford University, Stanford, CA 94305, USA
† Department of Radiology, Molecular Imaging Program, Stanford University, Stanford, CA 94305, USA
‡Department of Radiology, Stanford University Medical Center, Stanford University, Stanford, CA 94305, USA

***Abstract*—A scanning acoustic and photoacoustic microscope is demonstrated. The laser illumination and ultrasound detection in the system are co-axial. Pulsed light from a tunable optical parametric oscillator (OPO) laser is delivered to the scan tank via optical fiber. Multiple acoustic transducers with center frequencies varying from 5 MHz to 25 MHz are utilized. Images of a pig kidney (ex vivo) and a microcalcification phantom (eggshells embedded in agarose) are shown.**

## I. Introduction

Scanning acoustic microscopy has been used to study the elasticity of cells, thus giving insight into the mechanical structure of tissue [1]. Optical imaging techniques such as confocal microscopy provide functional information about cells, however, they cannot image at depths more than a few millimeters in tissue due to the scattering of light. Ultrasound scattering is two to three orders of magnitude weaker than optical scattering in biological tissue [2]. Hence, ultrasound can provide better resolution than pure optical imaging at depths of more than a few millimeters. In photoacoustic imaging, the target is illuminated with short laser pulses that generate acoustic pressure waves due to the thermoelastic effect. Photoacoustic imaging relies on absorbed light to provide contrast information and is thus less sensitive to the scattering of light. Therefore, photoacoustic imaging is able to combine the contrast information of optical imaging with the spatial resolution of acoustic imaging [3]. For this reason there has been great recent interest in photoacoustic microscopy [4]. A system that can perform both photoacoustic and acoustic imaging produces images that can provide mechanical as well as functional information. Furthermore, the ability to use optical excitation at different wavelengths enables spectroscopic analysis and the usage of smart background subtraction and multiplexing techniques in imaging.

In this work we report on the development of a scanning acoustic and photoacoustic microscope. This system can be used for tissue characterization, small animal imaging and characterization of photoacoustic contrast agents. This system also complements the ongoing efforts to build an array-detector based photoacoustic imaging system [5]. For this work the microscopy system was used to image a pig kidney (ex vivo) as well as a breast microcalcification phantom. The microcalcification phantom consisted of eggshell fragments embedded in an agarose gel.

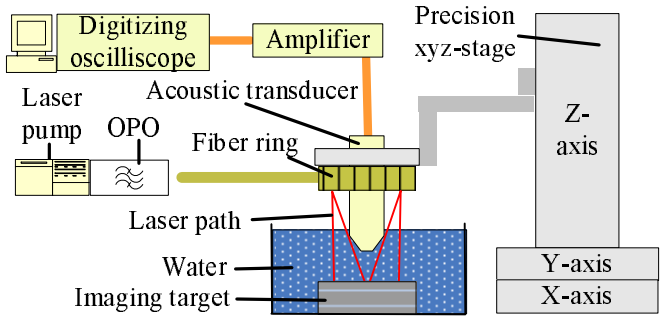


(a)

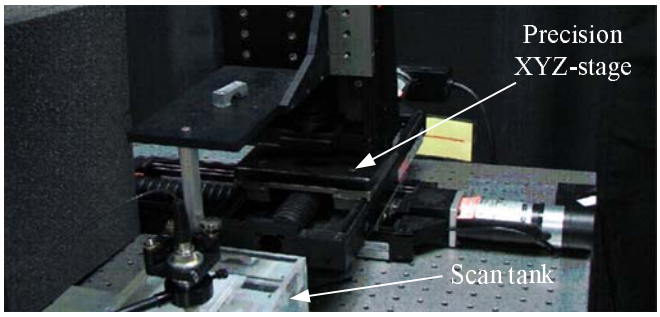


(b)

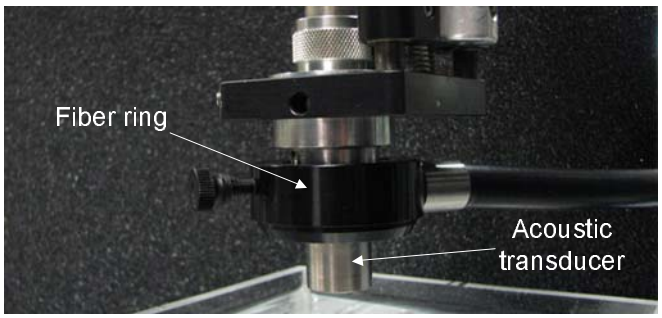


(c)

Fig. 1. Experimental setup: (a) Labeled schematic of setup (b) Photograph of setup (c) Transducer holder and fiber ring close up

## II. Experimental Setup

In the microscopy system (Fig. 1), the laser source is an optical parametric oscillator (OPO) pumped by a Q-switched Nd:YAG laser (Continuum SLIII-10). Laser pulses with a pulsewidth of 5 ns and repetition rate of 10 Hz are coupled into an optical fiber. The distal end of the fiber terminates in a fiber optic ring that is co-axial with the ultrasonic transducer as shown in (Fig. 1c). The transducer and the fiber optic ring are mounted on a precision xyz-stage that has a minimum step size of 1 $\mu$m (Fig. 1b). The movement of the xyz-stage is controlled by a Labview program. In photoacoustic mode, the sample is irradiated with laser pulses which induce acoustic waves that are detected by the ultrasound transducer. The sample is raster scanned to get a complete 3D image. Focused ultrasonic transducers ranging in center frequency from 5 MHz to 25 MHz (Panametrics) are used in the system. The scanning is repeated at different optical wavelengths ranging from 675 nm to 1050 nm. The photoacoustic signals received by the ultrasonic transducer are amplified by a low-noise amplifier and recorded by a digitizing oscilloscope. In pulse-echo mode, the laser is turned off, and a high-voltage spike-type electronic pulser is used to excite the ultrasonic transducer.

The photoacoustic and pulse-echo images are reconstructed as follows: The a-scan from each (x,y) position of the transducer is bandpass filtered and envelope detected before being combined to reconstruct a 3D intensity image of the target. The image is then log compressed according to the dynamic range desired. In the acoustic images, the intensity represents the acoustic reflectivity of the target while in the photoacoustic images, the intensity represents the optical absorption coefficient of the target. The photoacoustic and pulse-echo images are co-registered at the end.

TABLE I
Optical Characterization

| | |
|---|---|
| Wavelength, nm | 690 |
| Maximum Energy, mJ | 20.7 |
| Minimum Energy, mJ | 9.26 |
| Average Energy, mJ | 15.7 |
| Std Deviation, mJ | 2.34 |
| RMS Stability, % | 14.89 |
| PTP Stability, % | 72.80 |
| Rep rate, Hz | 9.98 |

TABLE II
Transducer characteristics

| Panametrics Transducers | | | |
|---|---|---|---|
| Model number | A309S | A319S | V324 |
| Center Frequency, MHz | 5.36 | 11.96 | 24.10 |
| 6 dB Bandwidth, MHz | 3.95 | 5.40 | 12.05 |
| Focal Length, mm | 25.53 | 19.02 | 27.10 |
| F number | 2.00 | 1.50 | 4.20 |
| Depth of focus, mm | 5.5 | 1.8 | 7.5 |

## III. Setup Characterization

The microscopy system was characterized, tested and verified before being used for experiments. Table I shows the optical power measurements of the laser at a sample wavelength of 690 nm. The fiber ring focuses the laser beam to a diameter of 1 cm at the point of imaging. Thus the average intensity of a laser pulse is below 20 mJ/cm$^2$ (within the ANSI safety standards [6]). Table II summarizes the measured characteristics of the three different acoustic transducers used in the experiment. Fig. 2 shows the 2-way insertion loss measurement for these same transducers. All the transducers are from Panametrics with a fixed focus. The overall system, including image reconstruction, was tested by performing an ultrasound scan of a United States quarter dollar coin and a photoacoustic scan of a printed Stanford logo. The Panametrics A319S transducer was used for these tests. Fig. 3 shows that the system is able to provide high quality acoustic images. In particular, Fig. 3b illustrates that even the bottom surface of the coin can be clearly imaged while the transducer is focused on the top surface of the coin. Fig. 4 confirms that the photoacoustic mode of the system is working. There is good agreement between the photograph (Fig. 4a) and the photoacoustic image (Fig. 4b).

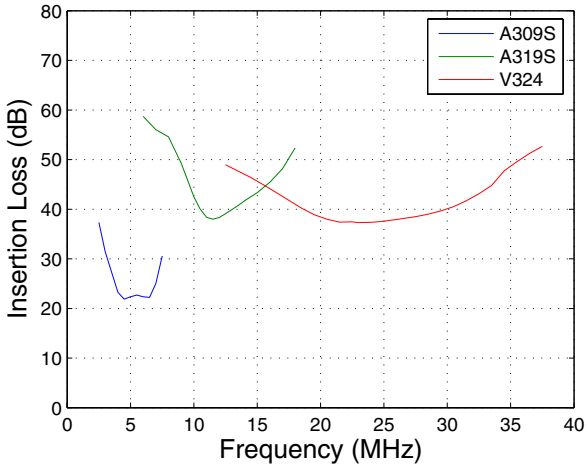


Fig. 2. 2-way insertion loss measurement of Panametrics transducers.

## IV. Results

### A. Microcalcification phantom

Agar based tissue mimicking phantoms containing eggshell fragments were imaged in photoacoustic and acoustic modes. The eggshell fragments embedded in agar are used to simulate breast microcalcifications [7]. Microcalcifications in the breast is a possible indicator of the onset of cancer. The Panametrics V324 transducer was used to scan this sample. Photoacoustic and acoustic images of this phantom are shown in Fig. 5 with a 30 dB dynamic range. These images are consistent with the photograph of the sample in Fig. 5b. The photoacoustic image shows more contrast than the pulse-echo image.

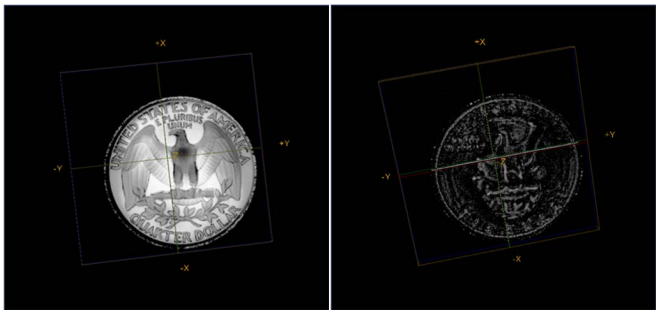

(a) (b)

Fig. 3. Pulse-echo images of a United States quarter dollar coin: (a) Top surface of coin, 25dB (b) Bottom surface of coin with focus of transducer still on top surface of coin, 25dB

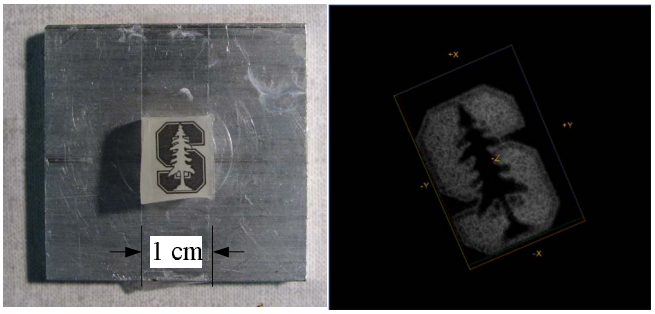


(a) (b)

Fig. 4. Printed Stanford logo phantom: (a) Photograph of Stanford logo phantom (b) Photoacoustic image of Stanford logo phantom, 25 dB

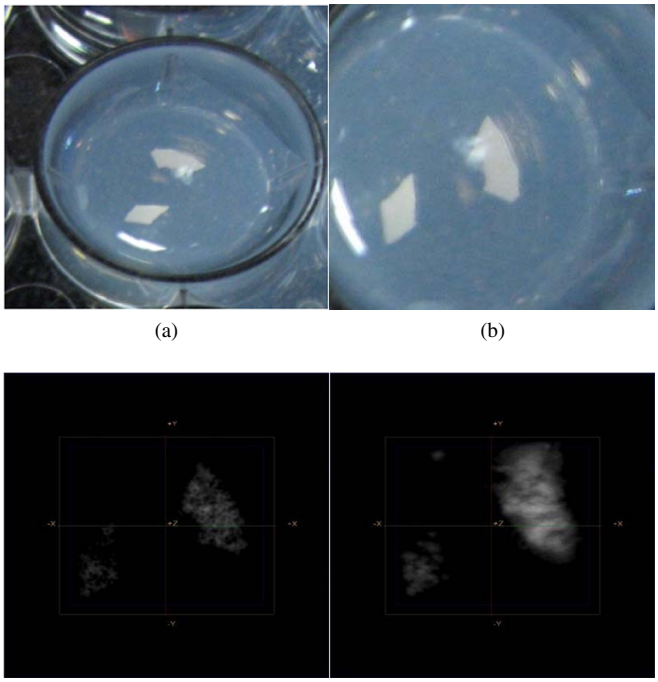

(a) (b) (c) (d)

Fig. 5. Images of eggshell fragments in agar gel: (a) Photograph of eggshell fragments in agar gel (b) Zoomed in photo of eggshell fragments (c) Pulse-echo image, 30 dB (d) Photoacoustic image, 30 dB

### *B. Pig kidney*

The system was also used to image a pig kidney ex vivo. A photograph of the cross-section of the pig kidney that was imaged is shown in Fig. 7a. The Panametrics V324 transducer was used to scan this sample. Sample pulse-echo and photoacoustic a-scans are shown in Fig. 6. These a-scans are unfiltered and are taken from the same spot in the sample. Note that the timescale in the photoacoustic a-scan is halved because the ultrasound is only acquired in receive mode. Acoustic and photoacoustic images are presented in Fig. 7b and Fig.7c respectively. The figures show that the acoustic and photoacoustic images provide complementary information. The capsule, cortex and medulla of the kidney are apparent in the pulse-echo image. The photoacoustic image shows the boundary of the renal hilum.

## V. Conclusion

In summary, a microscope that is able to image in both acoustic and photoacoustic modes has been demonstrated. The microscopy system has the capability to image at different acoustic frequencies as well as optical wavelengths. The system was fully characterized, tested and verified before being used. Acoustic and photoacoustic images of a breast microcalcification phantom and a pig kidney are presented in this work. For future work we intend to investigate the

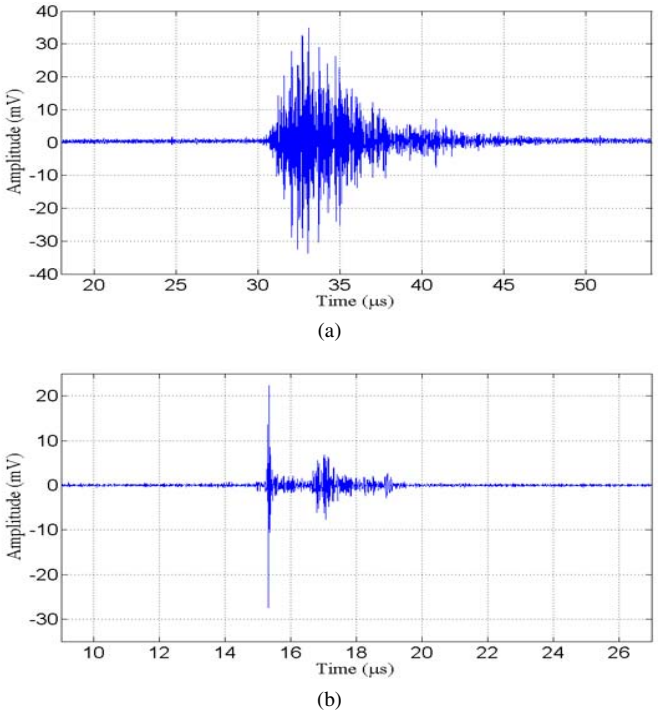


(a) (b)

Fig. 6. Sample A-scans from the pig kidney, taken from the same spot: (a) Pulse-echo a-scan (b) Photoacoustic a-scan

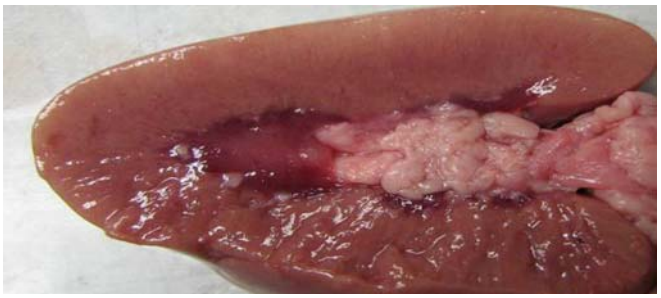

(a)

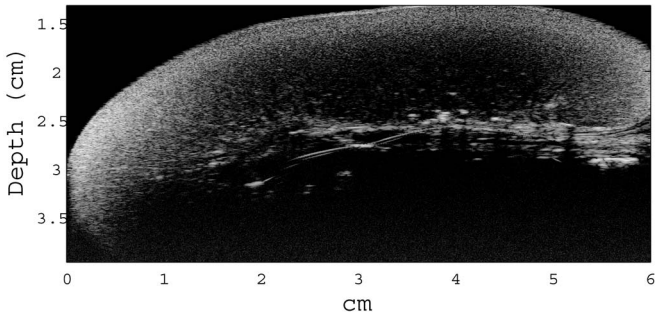


(b)

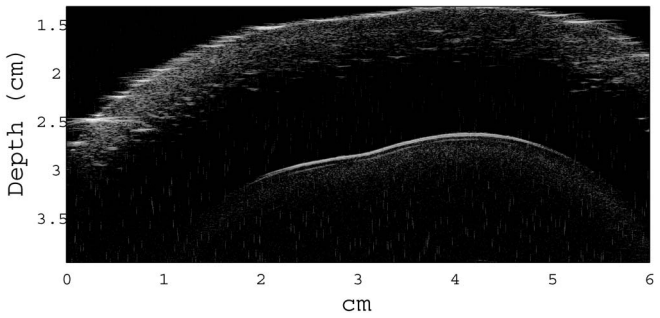


(c)

Fig. 7. Images of a pig kidney: (a) Photograph of the pig kidney showing approximately the cross-section that was scanned: (a) Pulse-echo image, 40 dB (b) Photoacoustic image, 40 dB

photoacoustic absorption spectra of real microcalcifications and the possible usage of contrast agents to enhance their detection. This system can also be used to perform further tissue characterization and small animal imaging.

## ACKNOWLEDGMENT

This work was supported by funds from Canon Inc. Larry Randall provided valuable support for machining the experimental equipment. Srikant Vaithilingam is supported by a P. Michael Farmwald Stanford Graduate Fellowship.

## REFERENCES

[1] J. Bereiter-Hahn, I. Karl, H. Lüers, and M. Vöth, "Mechanical basis of cell shape: investigations with the scanning acoustic microscope."

[2] F. A. Duck, *Physical Properties of Tissue - A Comprehensive Reference Book*. London: Academic Press, 1990.

[3] L. Wang, "Ultrasound-mediated biophotonic imaging: a review of acousto-optical tomography and photo-acoustic tomography," *Journal of Disease Markers*, vol. 19, pp. 123–138, 2004.

[4] H. Zhang, K. Maslov, G. Stoica, and L. Wang, "Functional photoacoustic microscopy for high-resolution and noninvasive in vivo imaging," *Nat. Biotechnol*, vol. 24, pp. 848–851, 2006.

[5] S. Vaithilingam, I. O. Wygant, S. Sifferman, X. Zhuang, Y.Furukawa, Ö. Oralkan, S. Keren, S. S. Gambhir, and B. T. Khuri-Yakub, "Tomographic photoacoustic imaging using capacitive micromachined ultrasonic transducer (cmut) technology," ser. IEEE Ultrasonics Symposium, Vancouver, Canada, Oct. 2006.

[6] *Safe use of lasers: ANSI Z136.1*, American National Standards Institute Std., 2000.

[7] S. Obenauer, K. Hermann, C. Schorn, M. Funke, U. Fischer, and E. Grabbe, "Full-field digital mammography: a phantom study for the detectability of simulated microcalcifications," *Fortschr Röntgenstr*, vol. 172, pp. 646–650, 2000.